

The box anomaly and radiative decays of $\eta(\eta')$ -mesons

M. A. Ivanov* and T. Mizutani

Department of Physics
Virginia Polytechnic Institute and State University
Blacksburg, VA 24061

July 19, 2018

Abstract

We report on a confined quark model calculation of the transition form factors for the radiative decays of $\eta(\eta') \rightarrow \gamma l^+ l^-$ and $\eta(\eta') \rightarrow \gamma \pi^+ \pi^-$. The η/η' mixing angle θ_P is determined from the set of data on the electromagnetic $\eta(\eta')$ decays. It is found that $\theta_P \sim -16.5^\circ$.

The analysis of the dipionic mass distribution in the decay $\eta' \rightarrow \gamma \pi^+ \pi^-$ confirms the existence of a non-resonant contribution which is the box anomaly.

PACS number(s): 12.39.-x, 12.39.Ki, 12.40.Vv, 11.30.Rd, 13.40.Gp, 13.40.Hq, 14.40.-n.

*Permanent address: Bogoliubov Laboratory of Theoretical Physics, Joint Institute for Nuclear Research, 141980 Dubna (Moscow Region), Russia

1 Introduction

The interest of studying the properties of the neutral pseudoscalar particles π^0 , η and η' is not weakened from the beginning of creation of unitary $SU(3)$ symmetry. One of the intriguing problems was the so-called "U(1)-problem" which was originally encountered by Glashow [1]. He considered extending $SU(3) \times SU(3)$ to $U(3) \times U(3)$ and found that if the extra U(1) axial symmetry was realized spontaneously, there would have to be an extra light pseudoscalar meson with mass compatible with pion (140 MeV). But the only flavor singlet meson is η' with a mass being equal to 958 MeV! After the advent of QCD, one could suggest that the anomaly associated with axial U(1) transformations might be used to provide a solution of U(1)-problem because of the divergence of axial current does not vanish in the chiral limit. However, the matter was found to be not so simple (see, for review [2]). Witten [3] found that the anomaly could be turned off as a number of quark colors goes to infinity ($N_c \rightarrow \infty$) and then the η' -meson would be considered as the Nambu-Goldstone boson. With finite N_c he suggested that the mass squared of the η' was proportional to $1/N_c$. Following this way, Veneziano [4] proposed a more explicit mechanism which was consistent with anomalous Ward identities and realized it by using the effective chiral Lagrangian incorporated explicitly $U_A(1)$ anomaly. The phenomenological implications of those Lagrangians to the $\eta - \eta'$ -mixing allowed one to get the mass formulas for the masses of η and η' and the mixing angle which reproduce the experimental values with quite reasonable accuracy.

The three-flavor Nambu-Jona-Lasinio (NJL) model with the instanton-induced six-quark effective interaction which incorporates effects of $U_A(1)$ anomaly has been developed to study the spectrum of low-lying mesons, the $\eta - \eta'$ -mixing, etc. [5].

The lattice calculations of the η' mass have been performed in [6] with taking into account U(1) gluon contributions which confirm that the η' owes its mass to the topological susceptibility.

One can say that the investigation of the internal structure of the neutral pseudoscalar (also vector) mesons is of great interest. As well known that very good probe of hadronic structure is the photon, for example, the study of electromagnetic form factors gives us the knowledge on the internal structure of charged particles. However, the genuine neutral particles like π^0 , η , η' mesons have no electromagnetic form factors because

of C-invariance. Therefore, it is needed to study the two-photon processes like $P \rightarrow \gamma\gamma$ ($P = \pi^0, \eta, \eta'$) with one or both photons being off mass shell to probe their structure.

One has to remark that theoretically the decay $\pi^0 \rightarrow \gamma\gamma$ with both of photons being on mass shell is defined by the Adler-Bell-Jackiw (ABJ) triangle anomaly whereas the gluon contribution from $U_A(1)$ anomaly should be taken into account under derivation of expression for $\eta'(\eta)\gamma\gamma$ coupling [7]. In many papers people do not use a such complication and just employ the parametrization of those amplitudes in terms of the decay constants $F_\pi, F_\eta, F_{\eta'}$, and the $\eta-\eta'$ mixing angle which are determined by fitting the relevant experimental data [8]. A precise relation has been established between these phenomenological parameters and those of the chiral expansion [9].

The more deep insight to the structure of neutral particle may be done by looking at the photon-dilepton decays $P \rightarrow \gamma l^+ l^-$ (and similar decays of the neutral vector mesons $V \rightarrow P l^+ l^-$ with V being ρ^0, ω, ϕ) (see, review [10]). These processes are determined by the transition form factor $F_{PVV}(q^2)$ in the time-like region of momentum transfer squared. Obviously, it is not enough to use the effective chiral lagrangians to obtain such form factor. It is needed to involve some assumptions on dynamics of such transitions like the vector dominance model (VDM) or quark models. The transition form factors in space-like region ($Q^2 = -q^2 \geq 0$) have been studied experimentally in the reaction $e^+e^- \rightarrow e^+e^-P$ and are planning to study in the photo and electroproduction of η' from nucleons and nuclei on CEBAF's energy using the "virtual" Primakoff effect [11].

Another processes which help to shed light on the structure of the $\eta(\eta')$ mesons are decays $\eta(\eta') \rightarrow \pi^+\pi^-\gamma$ which are described theoretically by both the box-anomaly and resonance contribution.. The phenomenolgical analysis of these processes have been done in paper [12].

To summarize this brief sketch, we would like to emphasize once more that many efforts have been devoted to describing the low-energy hadron physics in terms of effective chiral Lagrangians which include the Wess-Zumino anomaly [13]-[18]. There low-energy QCD is described in terms of mesonic degrees of freedom instead of those quarks and gluons with taking into account the underlying symmetries and anomalies of QCD. The hadronic verteces in the effective Lagrangians are structureless therefore the simple way to take into account the momentum dependence has been chosen by incorporating the vector mesons

either as massive Yang-Mills bosons or as the dynamical gauge bosons of a hidden local symmetry in the nonlinear chiral Lagrangians [15], [16].

We also note that the popular methods of QCD sum rules and lattice QCD are limited for timelike region. There are a few QCD-motivated quark models which incorporate quark degrees of freedom and allow one to describe many-particle processes both at spacelike and timelike regions. One of them [19] is based on the QCD Dyson-Schwinger equations with solution describing a confined quark, and another one [20], [21] is based on the phenomenological treatment of the mesons as $q\bar{q}$ states with the confinement ansatz to ensure the absence of quark production thresholds in the S-matrix elements of physical processes. Both of them have been successfully applied to describing the low-energy processes such as the reaction $\gamma\pi \rightarrow \pi\pi$. The salient feature of our confined quark approach [20], [21] is that all mesons (pseudoscalar, vector, scalar, etc.) are described as $q\bar{q}$ states by writing down the interaction Lagrangians and employing the compositeness condition to determine the meson-quark vertex coupling constants. The S-matrix elements are calculated in the lower order in the $1/N_c$ expansion which automatically includes the diagrams with intermediate resonances.

In the present article we report on a calculation of the transition form factors of the processes $P \rightarrow \gamma l^+ l^-$ and $V \rightarrow P l^+ l^-$ which are related to the study of momentum dependence of triangle anomaly, and the $\eta(\eta') \rightarrow \gamma\pi^+\pi^-$ -decays which are related to the box anomaly within a confined quark model. This is a continuation of study the momentum dependence of anomalous processes which we started in the paper [22].

2 Model

A confined quark model is specified by the interaction Lagrangian describing the transition mesons into quarks

$$L_I(x) = ig_P \bar{q}(x) P(x) \gamma^5 q(x) + g_V \bar{q}(x) V^\mu(x) \gamma^\mu q(x) + e A^\mu(x) \bar{q}(x) Q \gamma^\mu q(x) \quad (1)$$

with the lowest lying pseudoscalar and vector nonet meson matrices being equal to

$$P = \begin{pmatrix} \sqrt{\frac{1}{2}}\pi^0 + \sqrt{\frac{1}{6}}\eta_8 + \sqrt{\frac{1}{3}}\eta_1 & \pi^+ & K^+ \\ \pi^- & -\sqrt{\frac{1}{2}}\pi^0 + \sqrt{\frac{1}{6}}\eta_8 + \sqrt{\frac{1}{3}}\eta_1 & K^0 \\ K^- & \bar{K}^0 & -\sqrt{\frac{2}{3}}\eta_8 + \sqrt{\frac{1}{3}}\eta_1 \end{pmatrix}$$

$$V = \begin{pmatrix} \sqrt{\frac{1}{2}}\rho^0 + \sqrt{\frac{1}{6}}\omega_8 + \sqrt{\frac{1}{3}}\omega_1 & \rho^+ & K^{*+} \\ \rho^- & -\sqrt{\frac{1}{2}}\rho^0 + \sqrt{\frac{1}{6}}\omega_8 + \sqrt{\frac{1}{3}}\omega_1 & K^{*0} \\ K^{*-} & \bar{K}^{*0} & -\sqrt{\frac{2}{3}}\omega_8 + \sqrt{\frac{1}{3}}\omega_1 \end{pmatrix}$$

The physical fields η , η' , and ω , ϕ are defined in the standard manner by introducing the mixing angles as

$$\begin{aligned} \eta &= -\eta_1 \sin \theta_P + \eta_8 \cos \theta_P & \eta' &= \eta_1 \cos \theta_P + \eta_8 \sin \theta_P \end{aligned} \quad (2)$$

$$\phi = -\omega_1 \sin \theta_V + \omega_8 \cos \theta_V \quad \omega = \omega_1 \cos \theta_V + \omega_8 \sin \theta_V$$

so that their interaction with quarks may be written as

$$\begin{aligned} L_I^{\eta, \eta'} &= -ig_\eta \eta \left\{ \frac{\bar{u}\gamma^5 u + \bar{d}\gamma^5 d}{\sqrt{2}} \sin \delta_P + \bar{s}\gamma^5 s \cos \delta_P \right\} \\ &\quad + ig_{\eta'} \eta' \left\{ \frac{\bar{u}\gamma^5 u + \bar{d}\gamma^5 d}{\sqrt{2}} \cos \delta_P - \bar{s}\gamma^5 s \sin \delta_P \right\} \end{aligned} \quad (3)$$

$$\begin{aligned} L_I^{\omega, \phi} &= -g_\phi \phi^\mu \left\{ \frac{\bar{u}\gamma^\mu u + \bar{d}\gamma^\mu d}{\sqrt{2}} \sin \delta_V + \bar{s}\gamma^\mu s \cos \delta_V \right\} \\ &\quad + ig_\omega \omega^\mu \left\{ \frac{\bar{u}\gamma^\mu u + \bar{d}\gamma^\mu d}{\sqrt{2}} \cos \delta_V - \bar{s}\gamma^\mu s \sin \delta_V \right\} \end{aligned} \quad (4)$$

where $\delta = \theta - \theta_I$. The "ideal" mixing angle is equal to $\theta_I = \arctan(1/\sqrt{2}) = 35.3^\circ$.

The mixing angles are usually determined from the mass formular (quadratic or linear) [23]: $\theta_P^{\text{quad}} = -11^\circ$, $\theta_P^{\text{lin}} = -23^\circ$, and $\theta_V^{\text{quad}} = 39^\circ$, $\theta_V^{\text{lin}} = 36^\circ$. This means that θ_V is very close to θ_I , i.e. $\phi \approx s\bar{s}$ and we will use this value in what follows.

The Veneziano's model [4] which incorporates the explicit $U_A(1)$ anomaly gives $\theta_P = -18^\circ$.

In our model we use the experimental values of all hadron masses under calculations of matrix elements and consider the mixing angles defined by Eq. (2) as the adjustable parameters. We determine θ_P by fitting the available experimental data.

The meson-quark coupling constants g_M are defined by the *compositeness condition* meaning that the renormalization constants of the meson fields are equal to zero

$$Z_M = 1 - g_M^2 \Pi'_M(m_M^2) = 0. \quad (5)$$

Here Π'_M is the derivative of the meson mass operator and m_M is the physical meson mass. In other words, the equation (5) provides the right normalization of the charge form factor $F_M(0) = 1$. This could be readily seen from the Ward identity

$$g_M^2 \Pi'_M(p^2) = g_M^2 \frac{1}{2p^2} p^\mu \frac{\partial \Pi_M(p^2)}{\partial p^\mu} = g_M^2 \frac{1}{2p^2} p^\mu T_M^\mu(p, p) = F_M(0) = 1.$$

where $T_M^\mu(p, p')$ is the three-point function describing charge form factor.

Mesonic interactions in the QCM are defined by the closed quark loops

$$\int d\sigma_v \text{tr} \left[M(x_1) S_v(x_1 - x_2) \dots M(x_n) S_v(x_n - x_1) \right]. \quad (6)$$

Here,

$$S_v(x_1 - x_2) = \int \frac{d^4 p}{(2\pi)^4 i} e^{-ip(x_1 - x_2)} \frac{1}{v\Lambda - \not{p}} \quad (7)$$

is a quark propagator with the scale parameter Λ characterizing the size of the confinement, and the measure $d\sigma_v$, which is essential for quark confinement, is defined to provide the absence of singularities in Eq. (6) corresponding to the physical quark production:

$$\int \frac{d\sigma_v}{v - z} \equiv G(z) = a(-z^2) + zb(-z^2). \quad (8)$$

The shapes of the confinement functions $a(u)$ and $b(u)$, and the scale parameter Λ have been determined from the best model description of data in low-energy processes:

$$a(u) = 2 \exp(-u^2 - u) \quad b(u) = 2 \exp(-u^2 + 0.4u) \quad \Lambda = 460 \text{ MeV}, \quad (9)$$

which describe various basic constants quite well (see, [20], [21]).

The analytical expressions and numerical values for the meson-quark coupling constants from Eq. (5) are written down

$$g_P = 2\pi\sqrt{\frac{2}{3R_{PP}(\mu_P^2)}} = \begin{cases} 3.37 & \pi \\ 2.92 & \eta \\ 2.65 & \eta' \end{cases}$$

$$g_V = 2\pi\sqrt{\frac{1}{R_{VV}(\mu_V^2)}} = \begin{cases} 3.24 & \rho \\ 3.23 & \omega \\ 3.17 & \phi \end{cases}$$

We use the notation $\mu = m/\Lambda$ throughout. The structural integrals $R_{PP}(x)$ and $R_{VV}(x)$ are given in the Table I.

Also we have the possibility to investigate the consequences of the explicit $U_A(1)$ breaking in our approach. To do it, we may just assume that the octet and singlet coupling constants in the Lagrangian (1) are not equal each other

$$L_{81} = \frac{i}{\sqrt{2}}\bar{q}\left(g_8\eta_8\lambda^8 + g_1\eta_1\lambda^0\right)\gamma^5 q \quad (10)$$

where $\lambda^0 = \sqrt{2/3}I$. Using this Lagrangian in the compositeness condition (5) and defining the effective couplings of physical fields with quarks give

$$\begin{aligned} g_\eta^2 &\equiv g_8^2 \cos^2 \theta + g_1^2 \sin^2 \theta = \frac{1}{\Pi'_P(m_\eta^2)} \\ g_{\eta'}^2 &\equiv g_8^2 \sin^2 \theta + g_1^2 \cos^2 \theta = \frac{1}{\Pi'_P(m_{\eta'}^2)}. \end{aligned} \quad (11)$$

Then we introduce two new angles characterizing the $\eta - \eta'$ - mixing with taking into account the $U_A(1)$ -breaking:

$$\sin \theta_\eta = \frac{g_1}{g_\eta} \sin \theta \quad \sin \theta_{\eta'} = \frac{g_8}{g_{\eta'}} \sin \theta.$$

Thus the explicit $U_A(1)$ breaking gave us two different mixing angles which are determined by the η and η' masses through the compositeness condition and the initial mixing angle θ . Their numerical values are not much differ from this angle, for example, if $\theta = -11^\circ$

then $\theta_\eta = -9.9^\circ$ and $\theta_{\eta'} = -12.2^\circ$, if $\theta = -18^\circ$ then $\theta_\eta = -16^\circ$ and $\theta_{\eta'} = -20.2^\circ$. The available experimental data on the $\eta(\eta')$ -decays have too large uncertainties to distinguish these possibilities. So we will not consider the explicit $U_A(1)$ -breaking for the time being.

3 Radiative decays of neutral pseudoscalar and vector mesons

3.1 $P \rightarrow \gamma l^+ l^-$ and $V \rightarrow P l^+ l^-$ decays

The study of electromagnetic structure of neutral mesons ($P = \pi^0, \eta, \eta', V = \rho^0, \omega, \phi$) may be done in the two-photon processes: $P \rightarrow \gamma\gamma$, $P \rightarrow \gamma l^+ l^-$, $P \rightarrow l^+ l^-$, or in the processes with a change of C-parity of the mesons in the initial and final states: $V \rightarrow P l^+ l^-$ and $P \rightarrow V l^+ l^-$.

First, we give the necessary model-independent formulas (invariant matrix elements and differential distributions) which we use in our calculations.

(a) $P \rightarrow \gamma l^+ l^-$.

$$M(P \rightarrow \gamma l^+ l^-) = e^3 G_{P\gamma\gamma}(m_P^2, 0, q^2) \varepsilon^{\mu\nu\alpha_1\alpha_2} \epsilon^\nu q_1^{\alpha_1} q^{\alpha_2} \frac{1}{q^2} \bar{l} \gamma^\mu l$$

$$\frac{d\Gamma(P \rightarrow \gamma l^+ l^-)}{dq^2 \cdot \Gamma(P \rightarrow \gamma\gamma)} = \frac{2\alpha}{3\pi} \frac{1}{q^2} \sqrt{1 - \frac{4m_l^2}{q^2}} \left[1 + \frac{2m_l^2}{q^2}\right] \left[1 - \frac{q^2}{m_P^2}\right]^3 |F_P(q^2)|^2 \quad (12)$$

$$F_P(q^2) = G_{P\gamma\gamma}(m_P^2, 0, q^2) / G_{P\gamma\gamma}(m_P^2, 0, 0)$$

$$\Gamma(P \rightarrow \gamma\gamma) = \frac{\alpha^2 \pi}{4} m_P^3 G_{P\gamma\gamma}^2(m_P^2, 0, 0),$$

Here p ($p^2 = m_P^2$), q_1 ($q_1^2 = 0$), and q are the four-momentum of pseudoscalar, photon, and lepton pair, respectively, and ϵ^ν is the polarization vector of outgoing photon.

(b) $V \rightarrow P l^+ l^-$.

$$\begin{aligned}
M(V \rightarrow Pl^+l^-) &= e^2 G_{VP\gamma}(m_V^2, m_P^2, q^2) \varepsilon^{\mu\nu\alpha_1\alpha_2} \epsilon^\nu q_1^{\alpha_1} q^{\alpha_2} \frac{1}{q^2} \bar{l} \gamma^\mu l \\
\frac{d\Gamma(V \rightarrow Pl^+l^-)}{dq^2 \cdot \Gamma(V \rightarrow \gamma P)} &= \frac{\alpha}{3\pi} \frac{1}{q^2} \sqrt{1 - \frac{4m_l^2}{q^2}} \left[1 + \frac{2m_l^2}{q^2}\right] \cdot \\
&\quad \left[1 - \frac{q^2}{(m_V - m_P)^2}\right]^{3/2} \left[1 - \frac{q^2}{(m_V + m_P)^2}\right]^{3/2} |F_{VP}(q^2)|^2
\end{aligned} \tag{13}$$

$$F_{VP}(q^2) = G_{VP\gamma}(m_V^2, m_P^2, q^2) / G_{VP\gamma}(m_V^2, m_P^2, 0)$$

$$\Gamma(V \rightarrow P\gamma) = \frac{\alpha}{24} m_V^3 \left[1 - \frac{m_P^2}{m_V^2}\right]^3 G_{VP\gamma}^2(m_V^2, m_P^2, 0)$$

Here p ($p^2 = m_V^2$), q_1 ($q_1^2 = m_P^2$), and q are the four-momentum of vector, pseudoscalar meson, and lepton pair, respectively, ϵ^ν is the polarization vector of incoming vector meson.

The transition form factors $F_P(q^2)$ and $F_{VP}(q^2)$ define the internal structure of the neutral mesons and should be calculated dynamically.

In our approach they are defined by the diagrams in Fig. 1 for the decay $P \rightarrow \gamma l^+ l^-$ and similar diagrams for the decay $V \rightarrow Pl^+ l^-$.

We have

$$G_{P\gamma\gamma}(p^2, q_1^2, q^2) = g_{P\gamma\gamma}(p^2, q_1^2, q^2) + q^2 \sum_V g_{VP\gamma}(p^2, q_1^2, q^2) g_{V\gamma}(q^2) D_V(q^2) \tag{14}$$

$$G_{VP\gamma}(p^2, q_1^2, q^2) = g_{VP\gamma}(p^2, q_1^2, q^2) + q^2 \sum_{V'} g_{VPV'}(p^2, q_1^2, q^2) g_{V'\gamma}(q^2) D_{V'}(q^2) \tag{15}$$

Here the first term corresponds to the triangle diagram whereas the second to the vector meson pole diagram in Fig. 1. One should emphasize that in our approach the contribution from the pole diagram vanishes if the photon is on mass shell ($q^2 = 0$) as a consequence of gauge invariance.

The quantities appearing Eqs. (14-15) are written down

$$g_{P\gamma\gamma}(p^2, q_1^2, q_2^2) = \frac{g_P}{2\sqrt{2}\pi^2} \frac{1}{\Lambda} C_{P\gamma\gamma} R_{P\gamma\gamma}(p^2/\Lambda^2, q_1^2/\Lambda^2, q_2^2/\Lambda^2)$$

$$g_{VP\gamma}(p^2, q_1^2, q_2^2) = \frac{3g_P g_V}{8\pi^2} \frac{1}{\Lambda} C_{VP\gamma} R_{P\gamma\gamma}(p^2/\Lambda^2, q_1^2/\Lambda^2, q_2^2/\Lambda^2)$$

$$g_{V\gamma}(q^2) = \frac{g_V}{4\sqrt{2}\pi^2} C_{V\gamma} R_V(q^2/\Lambda^2)$$

We do not write the expressions for $g_{VPV'}$ because of we will consider the only decay $\omega \rightarrow \pi^0 \mu^+ \mu^-$. In this case $g_{\omega\pi^0\rho} = (3g_\pi g_\rho g_\omega / 2\sqrt{2}\pi^2) R_{P\gamma\gamma}(p^2/\Lambda^2, q_1^2/\Lambda^2, q_2^2/\Lambda^2)$.

The structural integrals and SU(3)-factors entering these expressions are given in Table I and II.

The Eqs. (14-15) may be written in the forms which are more convenient for comparison with the VDM approach:

$$G_{\pi^0\gamma\gamma}(p^2, q_1^2, q^2) = g_{\pi^0\gamma\gamma}(p^2, q_1^2, q^2) \left\{ 1 + q^2 \left[\frac{1}{2} C_\rho(q^2) + \frac{1}{2} C_\omega(q^2) \right] \right\}$$

$$G_{\eta\gamma\gamma}(p^2, q_1^2, q^2) = g_{\eta\gamma\gamma}(p^2, q_1^2, q^2) \cdot \left\{ 1 + q^2 \frac{3}{5 \sin \delta_P + \sqrt{2} \cos \delta_P} \cdot \left[\frac{3 \sin \delta_P}{2} C_\rho(q^2) + \frac{\sin \delta_P}{6} C_\omega(q^2) + \frac{\sqrt{2} \cos \delta_P}{3} C_\phi(q^2) \right] \right\}$$

$$G_{\eta'\gamma\gamma}(p^2, q_1^2, q^2) = g_{\eta'\gamma\gamma}(p^2, q_1^2, q^2) \cdot \left\{ 1 + q^2 \frac{3}{5 \cos \delta_P - \sqrt{2} \sin \delta_P} \cdot \left[\frac{3 \cos \delta_P}{2} C_\rho(q^2) + \frac{\cos \delta_P}{6} C_\omega(q^2) - \frac{\sqrt{2} \sin \delta_P}{3} C_\phi(q^2) \right] \right\}$$

where

$$C_V(q^2) = \frac{g_V^2}{4\pi} D_V(q^2) R_V(q^2/\Lambda^2) = \frac{R_V(q^2/\Lambda^2)}{R_{VV}(m_V^2/\Lambda^2)} D_V(q^2) \quad (16)$$

with D_V being a vector meson propagator.

The expression for the renormalized vector propagator obtained within our model [24] in one-loop approximation is written

$$D_V(q^2) = \frac{R_{VV}(m_V^2/\Lambda^2)}{m_V^2 R_V(m_V^2/\Lambda^2) - q^2 R_V(q^2/\Lambda^2)} \quad (17)$$

where the obvious equality (see, Table 1) $(xR_V(x))' = R_{VV}(x)$ provides the residue at $q^2 = m_V^2$ to be equal to one.

The imaginary part of the $\rho(\omega)$ -meson propagators is not very important for π and η decays but it should be taken into account somehow for η' decay. In our approach the imaginary part should appear as a result of summing up the two-loop diagrams. It will be proportional to the whole decay width of a vector meson, for example, for ρ -meson it reads $\Gamma_\rho(q^2) = m_\rho(g_{\rho\pi\pi}^2(q^2)/48\pi)[1 - 4m_\pi^2/q^2]^{3/2}\Theta(q^2 - 4m_\pi^2)$ where $g_{\rho\pi\pi}(q^2) = (3g_\pi^2 g_\rho/4\sqrt{2}\pi^2)R_{VPP}(q^2)$.

Then the vector propagator may be written as

$$D_V(q^2) = \frac{R_{VV}(m_V^2/\Lambda^2)}{m_V^2 R_V(m_V^2/\Lambda^2) - q^2 R_V(q^2/\Lambda^2) - im_V \Gamma_V R_{VV}(m_V^2)} \quad (18)$$

with Γ_V being the experimental value for vector meson decay. We drop out the q^2 dependence of decay width since it is the resonance region. The extra factor $R_{VV}(m_V^2)$ in denominator is introduced to provide the correct normalization of propagator at $q^2 = m_V^2$. Also we will use the same magnitude of width for ρ and ω mesons $\Gamma_V = 151$ MeV because of ω has too small width (about 8 MeV) to be seen in the experiments and its account theoretically will just give unpleasant extra pick. Of course, one drops ϕ -width because it is not important at energy less 1 GeV.

For comparison, we will use the simplified VDM-form for vector propagators

$$D_V(q^2) = \frac{1}{m_V^2 - q^2 - im_V \Gamma_V}. \quad (19)$$

We will discuss the numerical results for decay widths and the form factors in the final subsection.

3.2 $\eta(\eta') \rightarrow \pi^+ \pi^- \gamma$ decay

First, we give the model-independent expressions for invariant matrix element decay width and distributions of the $P \rightarrow \pi^+ \pi^- \gamma$ -decay ($P=\eta$ or η'):

$$M^\mu(P \rightarrow \pi^+ \pi^- \gamma) = e\varepsilon^{\mu\alpha\beta\nu} p_+^\alpha p_-^\beta q^\nu G_{P \rightarrow \pi^+ \pi^- \gamma}(s_1, s_2, s_3) \quad (20)$$

$$\Gamma(P \rightarrow \pi^+ \pi^- \gamma) = \frac{\alpha}{256\pi^2} \frac{1}{m_P^3} \int_{4m_\pi^2}^{m_P^2} ds_2 s_2 \int_{s_1^-}^{s_1^+} ds_1 (s_1^+ - s_1)(s_1 - s_1^-) |G_{P \rightarrow \pi^+ \pi^- \gamma}(s_1, s_2, s_3)|^2$$

Here, the kinematical variables s_i are defined as

$$s_1 = (q + p_+)^2 \quad s_2 = (p_- + p_+)^2 \quad s_3 = (q + p_-)^2, \quad s_1 + s_2 + s_3 = m_P^2 + 2m_\pi^2.$$

so that they vary in the intervals $4m_\pi^2 \leq s_2 \leq m_P^2$ and $s_1^- \leq s_1 \leq s_1^+$ where

$$s_1^\pm = m_\pi^2 + (1/2)(m_P^2 - s_2)[1 \pm \sqrt{1 - 4m_\pi^2/s_2}].$$

In our approach the matrix element of the decay $P \rightarrow \pi^+ \pi^- \gamma$ is defined by the diagrams in Fig. 2. The expression for $G_{P \rightarrow \pi^+ \pi^- \gamma}$ is written down

$$G_{P \rightarrow \pi^+ \pi^- \gamma}(s_1, s_2, s_3) = g_{P \rightarrow \pi^+ \pi^- \gamma}^{\text{box}}(s_1, s_2, s_3) + 2g_{P\rho\gamma}(s_2)g_{\rho\pi\pi}(s_2)D_\rho(s_2)$$

$$g_{P\rho\gamma}(s_2) = C_P \frac{1}{\Lambda} \frac{3g_P g_\rho}{4\pi^2} R_{PVV}(m_P^2/\Lambda^2, s_2/\Lambda^2, 0)$$

$$g_{P \rightarrow \pi^+ \pi^- \gamma}^{\text{box}}(s_1, s_2, s_3) = C_P \frac{1}{\Lambda^3} \frac{3g_\pi^2 g_P}{4\pi^2 \sqrt{2}} R_\square(s_1/\Lambda^2, s_2/\Lambda^2, s_3/\Lambda^2)$$

$$R_\square(s_1, s_2, s_3) = \int d^4\alpha \delta(1 - \sum_{i=1}^4 \alpha_i) \{ -a'(-D_4^{-+\gamma}) + a'(-D_4^{+\gamma-}) - a'(-D_4^{\gamma-+}) \}$$

where

$$\begin{aligned} D_4^{-+\gamma} &= \alpha_3 \alpha_4 m_P^2 + \alpha_2(\alpha_1 + \alpha_3)m_\pi^2 + \alpha_1 \alpha_3 s_2 + \alpha_2 \alpha_4 s_1 \\ D_4^{+\gamma-} &= \alpha_2 \alpha_3 m_P^2 + (\alpha_3 \alpha_4 + \alpha_1 \alpha_2)m_\pi^2 + \alpha_1 \alpha_3 s_3 + \alpha_2 \alpha_4 s_1 \\ D_4^{\gamma-+} &= \alpha_1 \alpha_2 m_P^2 + \alpha_3(\alpha_2 + \alpha_4)m_\pi^2 + \alpha_1 \alpha_3 s_3 + \alpha_2 \alpha_4 s_2 \end{aligned}$$

The group coefficient C_P is equal to $-\sin \delta_P$ for η and $\cos \delta_P$ for η' .

One trivially finds that $R_\square(0, 0, 0) = 1/3$. In the physical region the box-contribution varies very slowly around this value so that we may approximate R_\square by this value with quite good accuracy in the calculations.

This gives the following formula for the decay width

$$\Gamma(P \rightarrow \pi^+ \pi^- \gamma) = \frac{\alpha}{12\pi^2} \int_{2m_\pi}^{m_P} dm E_\gamma^3 P_\pi^3 |G_{P \rightarrow \pi^+ \pi^- \gamma}^{(0)}(m^2)|^2. \quad (21)$$

with $E_\gamma = (m_P^2 - m^2)/2m_P$ and $P_\pi = (1/2)\sqrt{m^2 - 4m_\pi^2}$ being the photon energy in the ingoing meson rest system and the pion momentum in the dipion rest system, respectively. The label (0) upstairs G means that we use $R_\square = 1/3$ in the whole physical region.

The effective mass spectrum of the $\pi^+ \pi^-$ system is defined as

$$\frac{d\Gamma}{dm_{\pi\pi}} = \frac{\alpha}{12\pi^2} E_\gamma^3 P_\pi^3 |G_{\eta\pi^+\pi^-\gamma}^{(0)}(m_{\pi\pi}^2)|^2. \quad (22)$$

The photon energy spectrum is defined as

$$\frac{d\Gamma}{dE_\gamma} = \frac{\alpha}{24\pi^2} \frac{1}{\sqrt{s_2}} E_\gamma^3 P_\pi^3 |G_{\eta\pi^+\pi^-\gamma}^{(0)}(s_2)|^2. \quad (23)$$

with $s_2 = m_P(m_P - 2E_\gamma)$.

We will discuss the numerical results in the final subsection.

3.3 Discussion of the numerical results

The dependence of the ratios of the theoretical values of decay widths to their experimental averages on the mixing angle are shown in Fig. 3a Fig. 3b for the vector propagator shape described by Eq. (18) and Eq. (19), respectively. Visually, one can see that the value of the mixing angle $\theta_P = -16.5^\circ$ in Fig. 3a seems may give quite reasonable coincidence with the experimental data except the decay $\eta \rightarrow \pi\pi\gamma$ which theoretical value is 1.5 times larger than the average experimental one. One has to note that the value $\theta_P = -16.5^\circ$ is supported by two recent theoretical analysis: (1) $\eta, \eta' \rightarrow \gamma\gamma^*$ and $D_s \rightarrow \eta l\nu/\eta' l\nu$ which gives $\theta_P = -16.7^\circ \pm 2.8^\circ$ [25], and (2) J/ψ decays into a vector and pseudoscalar meson which gives $\theta_P = -16.9^\circ \pm 1.7^\circ$ [26].

First, we discuss the decays $\eta(\eta') \rightarrow \gamma\mu^+\mu^-$ and $\omega \rightarrow \pi^0\mu^+\mu^-$. The transition form factors described the observable spectra Eqs. (12-13) have been parametrized in the pole approximation [10] as

$$F_\eta(q^2) = \frac{1}{1 - q^2/\Lambda_\eta^2} \quad \Lambda_\eta = 0.72 \pm 0.09 \text{ GeV}, \quad (24)$$

$$F_{\omega\pi}(q^2) = \frac{1}{1 - q^2/\Lambda_\omega^2} \quad \Lambda_\omega = 0.65 \pm 0.03 \text{ GeV}. \quad (25)$$

As it is seen from Eqs. (24-25) a value of the characteristic mass, Λ , agrees well with vector dominance ($m_\rho = 0.77 \text{ GeV}$) for η -decay, and differs from those by four standard deviations for ω -decay. Our form factor (see, Fig. 4) goes slightly lower than the curve fitted the experimental data but it is still within the experimental uncertainties. The behavior of $\omega - \pi$ -form factor (see, Fig. 5) almost coincides with the fitting curve.

The behavior of the form factor describing the $\eta' \rightarrow \gamma\mu^+\mu^-$ decay is more interesting since the ρ^0 and ω poles occur in the physical region allowed for the muon pair spectrum. Experimental data on the η' -meson transition form factor, the VDM predictions with taking into account the ρ -meson decay width in the vector propagators, and the results of our calculations are shown in Fig. 6. A more detailed analysis is difficult to perform because of poor statistics.

Now let us discuss the decay $\eta' \rightarrow \gamma\pi^+\pi^-$ and related process $\eta' \rightarrow \rho^0\gamma$. There are lots of experiments devoted to the study of these decays [29]-[39]. Most of them are looking at the effective mass spectrum for the $\pi^+\pi^-$ system in the decay $\eta' \rightarrow \pi^+\pi^-\gamma$ (see, Fig. 7). It was shown in [39] that an attempt to fit the distribution in the framework of the cascade decay model $\eta' \rightarrow \rho^0\gamma$, $\rho^0 \rightarrow \pi^+\pi^-$ with simple choice of the vector propagator

$$\frac{dN}{dm_{\pi\pi}} \propto \frac{E_\gamma^3 P_\pi^3 m_{\pi\pi}^3}{(m_{\pi\pi}^2 - m_\rho^2)^2 + m_\rho^2 \Gamma_\rho^2}$$

with Γ_ρ being the "dynamical" width of ρ -meson is not successful because of the distribution obtained in experiment is much harder than the theoretical one. It was needed to assume that either the propagator form should be modified significantly without reasonable theoretical justifications or a nonresonance process gives significant contribution to this decay. The last assumption was realized [39] by modelling the distribution by the following form

$$\frac{dN}{dm_{\pi\pi}} \propto E_\gamma^3 P_\pi^3 m_{\pi\pi}^3 \left| \frac{1}{m_{\pi\pi}^2 - m_\rho^2 + im_\rho \Gamma_\rho} + \frac{\xi e^i \alpha}{m_{\eta'}^2} \right|^2.$$

As a result of fitting the experimental spectrum it was found that $\xi = 2.78 \pm 0.46$ and $\alpha = -1.07 \pm 0.08$.

Recent measurements of the $\pi^+\pi^-$ mass spectrum in the decay $\eta' \rightarrow \pi^+\pi^-\gamma$ with the Crystal Barrel detector [40] also confirmed the existence of a non-resonant coupling $\pi^+\pi^-\gamma$. We plot their data on Fig. 7a and compare them with our results and VDM prediction. It is readily seen that our results coincide quite well with the experimental data whereas the VDM predictions are significantly above them up to the resonant region.

The existence of the non-resonant contribution clearly comes from the existence of the box anomaly in chiral theory. One of the attempts to incorporate vector mesons in the chiral Lagrangian has been done in [16]. It was found that the amplitude of the decay $\eta \rightarrow \pi^+\pi^-\gamma$ is given by

$$M(\eta \rightarrow \pi^+\pi^-\gamma) = \frac{e}{4\pi^2 F_\pi^2} \epsilon^{\mu\nu\alpha\beta} p_\mu^+ p_\nu^- q_\alpha \varepsilon_\beta \left[\frac{1}{2} - \frac{3}{2} \frac{m_\rho^2}{m_\rho^2 - p_\rho^2} \right] \left[\frac{1}{\sqrt{3} f_8} \cos \theta - \sqrt{\frac{2}{3}} \frac{1}{f_0} \sin \theta \right] \quad (26)$$

where $f_8 = 1.25F_\pi$ and $f_0 = 1.04F_\pi$. A numerical result for the decay width obtained with $\theta = -20.6$ was $\Gamma(\eta \rightarrow \pi^+\pi^-\gamma) = 62$ eV which is close to the experiment $\Gamma_{\text{expt}} = 58 \pm 6$ eV. The direct generalization of this model for η' -decay by adding the imaginary part like $im_\rho\Gamma_\rho$ to the denominator of propagator and replacing $\cos \theta$ to $\sin \theta$ and $\sin \theta$ to $-\cos \theta$, respectively, gives the spectrum and the decay width listed in Fig. 7b in a agreement with the experimental data and our results.

Now we discuss the $\eta \rightarrow \pi^+\pi^-\gamma$ -decay. From the theoretical point of view this is simpler than the η' -decay since it is up to the resonance region. But experimental data are very poor, actually, there are only two experimental papers discussing this issue [28] and [27] where the γ -ray energy spectrum was measured. To compare the theoretical results with the experimental data, two forms of function $f(s)$ entering to the matrix element $M(\eta \rightarrow \pi^+\pi^-\gamma) \propto f(s) \varepsilon^{\mu\nu\alpha\beta} \epsilon_\gamma^\mu p_\gamma^\nu p_+^\alpha p_-^\beta$ have been used [28]: $f(s) = 1$ and $f(s) = m_\rho^2/(m_\rho^2 - s)$. The efficiency used in this procedure has not been given in explicit form. We are able to reproduce the results of the paper [28] with the efficiency function chosen in the form

$$\text{eff}(E_\gamma) = E_\gamma^a (E_\gamma^{(0)} - E_\gamma)^b \quad (27)$$

where $a = b = 1.1$. Using this efficiency function we recalculate the experimental data according to

$$\text{corrected data} = \text{data}/\text{eff}(E_\gamma)$$

and put them in Fig. 7a and Fig. 7b. One can see that the theoretical results from QCM, VDM, and the chiral approach implemented VDM [16] coincide each other and fit very well the experimental data. Finally we summarize our predictions for the rates of radiative decays of η and η' mesons in Table III.

ACKNOWLEDGMENTS

This work was supported in part by the United States Department of Energy under Grant No. DE-FG-ER40413.

References

- [1] S.L. Glashow, in: Hadrons and their interactions, Inter. School of Subnuclear Physics, Erice, 1967, ed. A.Zichichi (Academic Press, New York, 1968) p.83.
- [2] G.A. Christos, Phys.Rep. **116**, 251 (1984).
- [3] E. Witten, Nucl.Phys. **B156**, 269 (1979).
- [4] G. Veneziano, Nucl.Phys. **B159**, 213 (1979);
P. Di Vecchia and G. Veneziano, Nucl.Phys. **B171**, 253 (1980).
- [5] T. Hatsuda and T. Kunihiro, Phys.Rep. **247**, 221 (1994);
S. Klimt, M. Lutz, U. Vogl and W. Weise, Nucl.Phys. **A516**, 429 (1990);
M. Takizawa, K. Tsushima, Y. Kohyama and K. Kubodera, Nucl.Phys. **A507**, 611 (1990);
V. Bernard, R.L. Jaffe and U.-G. Meissner, Nucl.Phys. **B308**, 753 (1988);
R. Alkofer and H. Reinhardt, Z.Phys. **C45**, 275 (1989);
Yu.L. Kalinovsky and M.K. Volkov, Mod.Phys.Lett. **A9**, 993 (1994).
- [6] G. Kilcup, In the Proceedings of the workshop on the structure of the η' meson, New Mexico State University and CEBAF, Las Cruces, New Mexico, March 8-9, 1996.
- [7] G.M. Shore and G. Veneziano, Nucl.Phys. **B381**, 3 (1992).
- [8] F.J. Gilman and R. Kauffman, Phys.Rev. **D36**, 2761 (1987);
A.V. Kisselev and V.A.Petrov, Z.Phys. **C58**, 595 (1993).
- [9] B. Moussallam, Phys.Rev. **D51**, 4939 (1995).
- [10] L.G. Landsberg, Phys. Rep. **128**, 301 (1985).
- [11] R.M. Davidson, In the Proceedings of the workshop on the structure of the η' meson, New Mexico State University and CEBAF, Las Cruces, New Mexico, March 8-9, 1996.
- [12] M. Benayoun, Ph. Leruste, L. Montanet, and J.-L. Narjoux, Z.Phys. **C65**, 399 (1995).
- [13] J. Gasser and H. Leutwyler, Ann. Phys. (NY) **158**, 142 (1984); Nucl. Phys. **B250**, 465 (1985).
- [14] J.F. Donoghue, B.R. Holstein and Y-C.R. Lin, Phys. Rev. Lett. **55**, 2766 (1985).

- [15] U.-G. Meissner, Phys. Rep. **161**, 213 (1988).
- [16] C. Picciotto, Phys. Rev. **D45**, 1569 (1992).
- [17] J. Bijnens, A. Bramon, F. Cornet, Phys.Lett. **B237**, 488 (1990).
- [18] B.R. Holstein, hep-ph/9304201 (1993).
- [19] R. Alkofer and C.D. Roberts, Phys.Lett. **B369**, 101 (1996);
C.D. Roberts, Nucl. Phys. **A605**, 475 (1996).
- [20] G.V. Efimov and M.A. Ivanov, The Quark Confinement Model of Hadrons,
(IOP Publishing, Bristol & Philadelphia, 1993).
- [21] M.A. Ivanov and T. Mizutani, Phys. Rev. **D45**, 1580 (1992).
- [22] M.A. Ivanov and T. Mizutani, Phys.Rev. **D53**, 1470 (1996).
- [23] Review of Particle Properties, Phys.Rev. **D54**, 1 (1996).
- [24] G.V. Efimov and M.A. Ivanov, Int.Jour.Mod.Phys. **A4**, 2031 (1989).
- [25] V.V. Anisovich *et al.*, Phys.Lett. **B404**, 166 (1997).
- [26] A. Bramon, R. Escribano, M.D. Scadron, Phys.Lett. **B403**, 339 (1997).
- [27] M. Gormley *et al.*, Phys.Rev. **D2**, 501 (1970).
- [28] J.G. Layter *et al.*, Phys.Rev. **D7**, 2565 (1973).
- [29] [**Brookhaven**] M. Aguilar-Benitez *et al.*, Phys.Rev.Lett. **25**, 1635 (1970).
- [30] [**Brookhaven**] S.M. Jacobs *et al.*, Phys.Rev. **D8**, 18 (1973).
- [31] [**Brookhaven**] J.S. Danburg *et al.*, Phys.Rev. **D8**, 3744 (1973).
- [32] [**JADE Coll.**] L.W. Bartel *et al.*, Phys.Lett. **B113**, 190 (1982).
- [33] [**CELLO Coll.**] H.J. Behrend *et al.*, Phys.Lett. **B114**, 378 (1982).
- [34] [**PLUTO Coll.**] Ch. Berger *et al.*, Phys.Lett. **B142**, 125 (1984).
- [35] [**TASSO Coll.**] M. Althoff *et al.*, Phys.Lett. **B147**, 487 (1984).
- [36] [**TPC/ $\gamma\gamma$ Coll.**] H. Aihara *et al.*, Phys.Rev. **D35**, 2650 (1987).
- [37] [**ARGUS Coll.**] H. Albrecht *et al.*, Phys.Lett. **B199**, 457 (1987).
- [38] [**MARK II Coll**] F. Butler *et al.*, Phys.Rev. **D42**, 1368 (1990).

- [39] [**Lepton F Coll.**] S.I. Bityukov *et al.*, Z.Phys. **C50**, 451 (1991).
- [40] **Crystal Barrel Coll.** A. Abele *et al.*, Phys. Lett. **B402**, 195 (1997)

Table I. Variuos functions entering the QCM calculations of meson vertecies. Functions $a(u)$ and $b(u)$ characterize the confined quark propagator Eq. (8-9).

$R_{PP}(x) = B_0 + \frac{x}{4} \int_0^1 dub(-\frac{xu}{4}) \frac{(1-u/2)}{\sqrt{1-u}}$
$R_{VV}(x) = B_0 + \frac{x}{4} \int_0^1 dub(-\frac{xu}{4}) \frac{(1-u/2+u^2/4)}{\sqrt{1-u}}$
$R_V(x) = B_0 + \frac{x}{4} \int_0^1 dub(-\frac{xu}{4}) (1+u/2) \sqrt{1-u}$
$R_{VPP}(x) = B_0 + \frac{x}{4} \int_0^1 dub(-\frac{xu}{4}) \sqrt{1-u}$
$R_{PVV}(x, y, z) = \int d^3\alpha \delta(1 - \sum_1^3 \alpha_i) a(-\alpha_1\alpha_2x - \alpha_1\alpha_3y - \alpha_2\alpha_3z)$
$R_{PVV}(x, y, 0) = (xR_{PVV}(x, 0, 0) - yR_{PVV}(y, 0, 0))/(x - y)$
$R_{PVV}(x, 0, 0) = \frac{1}{4} \int_0^1 dua(-\frac{xu}{4}) \ln\left(\frac{1+\sqrt{1-u}}{1-\sqrt{1-u}}\right)$
$A_0 = \int_0^\infty dua(u) = 1.09 \quad B_0 = \int_0^\infty dub(u) = 2.26$

Table II. The SU(3)-factors entering the calculations of $P \rightarrow \gamma\gamma$ ($P \rightarrow \gamma l^+ l^-$);
 $V \rightarrow P\gamma$ ($V \rightarrow Pl^+ l^-$), $P \rightarrow V\gamma$; and $V \rightarrow \gamma \rightarrow l^+ l^-$ decays.

$C_{P\gamma\gamma} = 3\text{tr}(\lambda^P Q^2)$	P
1	π^0
$-(5 \sin \delta_P + \sqrt{2} \cos \delta_P)/3$	η
$(5 \cos \delta_P - \sqrt{2} \sin \delta_P)/3$	η'

$C_{VP\gamma} = \text{tr}(Q\{\lambda^P, \lambda^V\})$	$VP\gamma$
2/3	$\rho\pi\gamma$
2	$\omega\pi\gamma$
$-2 \sin \delta_P$	$\rho\eta\gamma$
$-(2/3) \sin \delta_P$	$\omega\eta\gamma$
$-(4/3) \cos \delta_P$	$\phi\eta\gamma$
$2 \cos \delta_P$	$\rho\eta'\gamma$
$(2/3) \cos \delta_P$	$\omega\eta'\gamma$
$-(4/3) \sin \delta_P$	$\phi\eta'\gamma$

$C_{V\gamma} = \text{tr}(\lambda^V Q)$	V
1	ρ^0
1/3	ω^0
$\sqrt{2}/3$	ϕ

Table III. Comparison of our predictions for radiative decay widths of neutral pseudoscalar and vector mesons with the available experimental data. Results are given for the $\eta - \eta'$ -mixing angle $\theta_P = -16.5^\circ$.

	QCM	Expt.
$\pi^0 \rightarrow \gamma\gamma$, eV	7.2	7.7 ± 0.6
$\eta \rightarrow \gamma\gamma$, KeV	0.45	0.46 ± 0.04
$\eta' \rightarrow \gamma\gamma$, KeV	4.2	4.26 ± 0.19
$\rho^0 \rightarrow \eta\gamma$, KeV	38	57 ± 12
$\eta \rightarrow \mu^+\mu^-\gamma$, eV	0.35	0.37 ± 0.06
$\eta \rightarrow \pi^+\pi^-\gamma$, eV	92	58 ± 6
$\eta' \rightarrow \mu^+\mu^-\gamma$, KeV	0.014	0.021 ± 0.007
$\eta' \rightarrow \pi^+\pi^-\gamma$, KeV	47	56 ± 9
$\eta' \rightarrow \rho^0\gamma$, KeV	38	61 ± 8
$\omega \rightarrow \pi\gamma$, KeV	590	716 ± 51
$\omega \rightarrow \pi\mu^+\mu^-$, KeV	0.49	0.81 ± 21

Fig. 1. The $P \rightarrow \gamma l^+ l^-$ decay.

Fig. 2. The $P \rightarrow \pi^+ \pi^- \gamma$ decay.

Fig. 3. The dependence of ratios of theoretical values for the radiative decays of η and η' mesons to their experimental averages on the mixing angles calculated with the shape of vector meson propagators defined by (a) Eq. (18), and (b) Eq. (19).

Fig. 4. The form factor of $\eta \rightarrow \gamma \mu^+ \mu^-$ decay.

Fig. 5. The form factor of $\omega \rightarrow \pi^0 \mu^+ \mu^-$ decay.

Fig. 6. The form factor of $\eta' \rightarrow \gamma \mu^+ \mu^-$ decay.

Fig. 7. The mass spectrum of $\eta' \rightarrow \gamma \pi^+ \pi^-$ decay:

(a) QCM and VDM (b) Chiral model [16] and VDM.

Fig. 8. The photon energy spectrum of $\eta \rightarrow \gamma \pi^+ \pi^-$ decay:

(a) QCM and VDM, (b) Chiral model [16] and VDM.

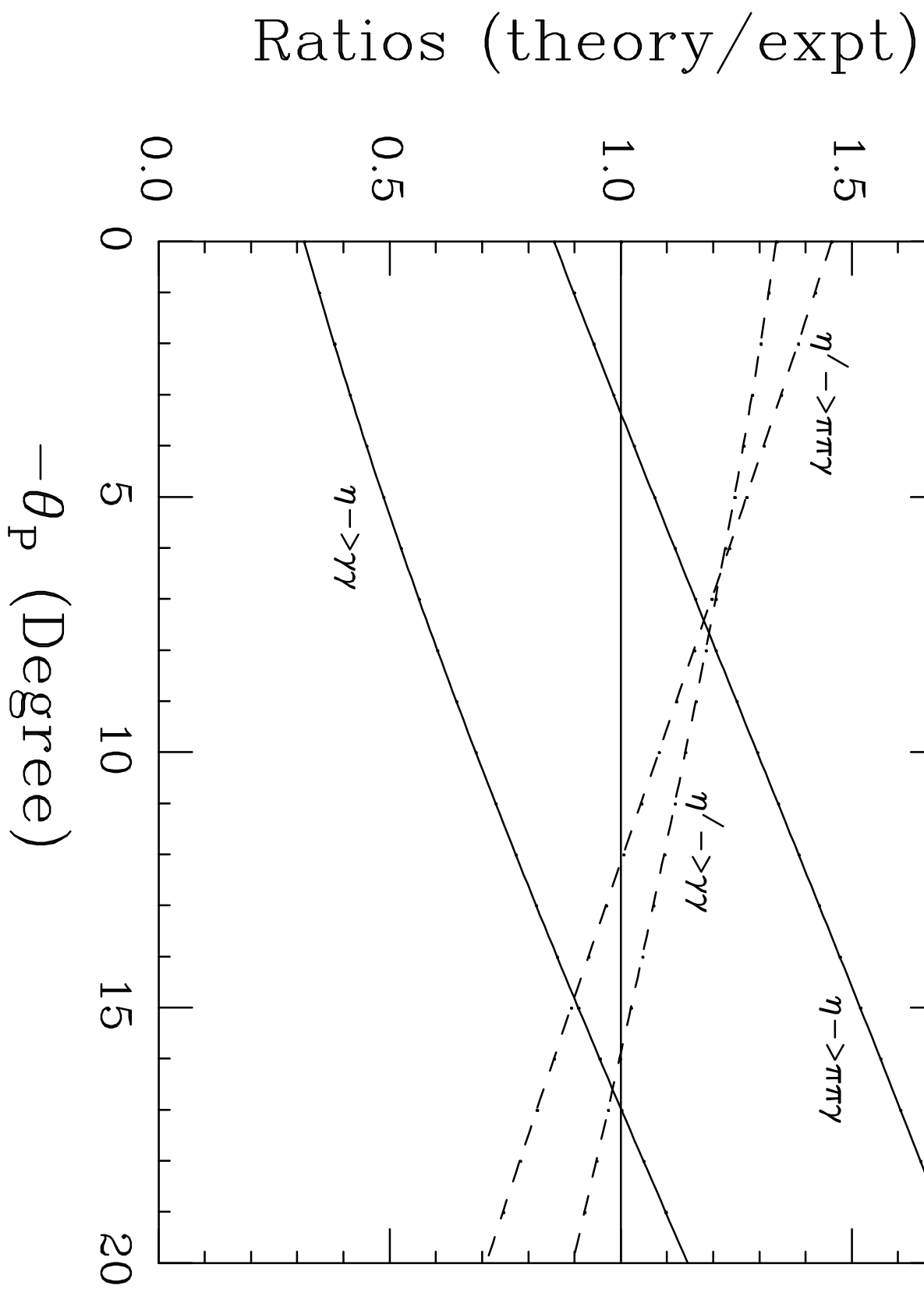


Fig. 3a

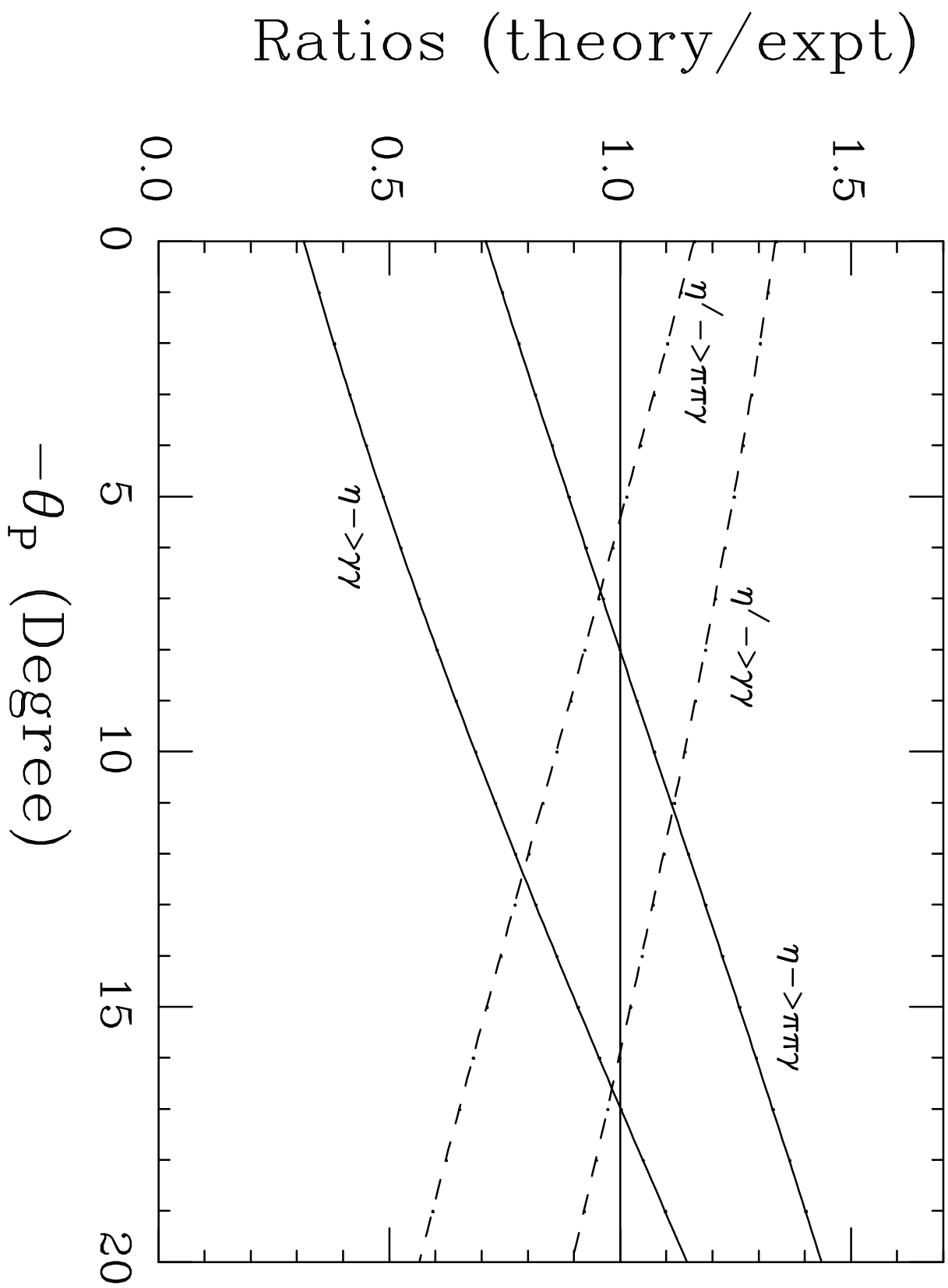


Fig. 3b

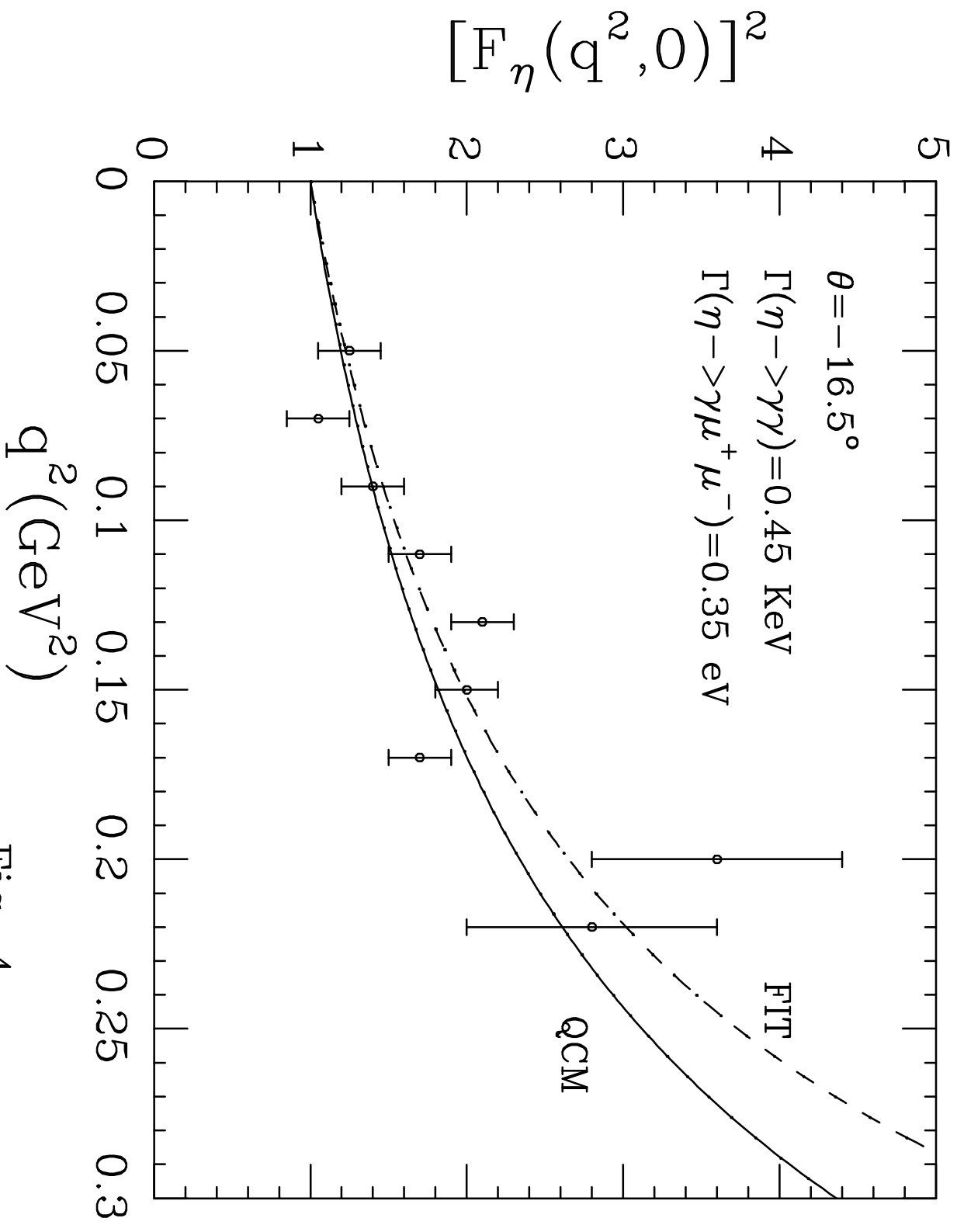


Fig. 4

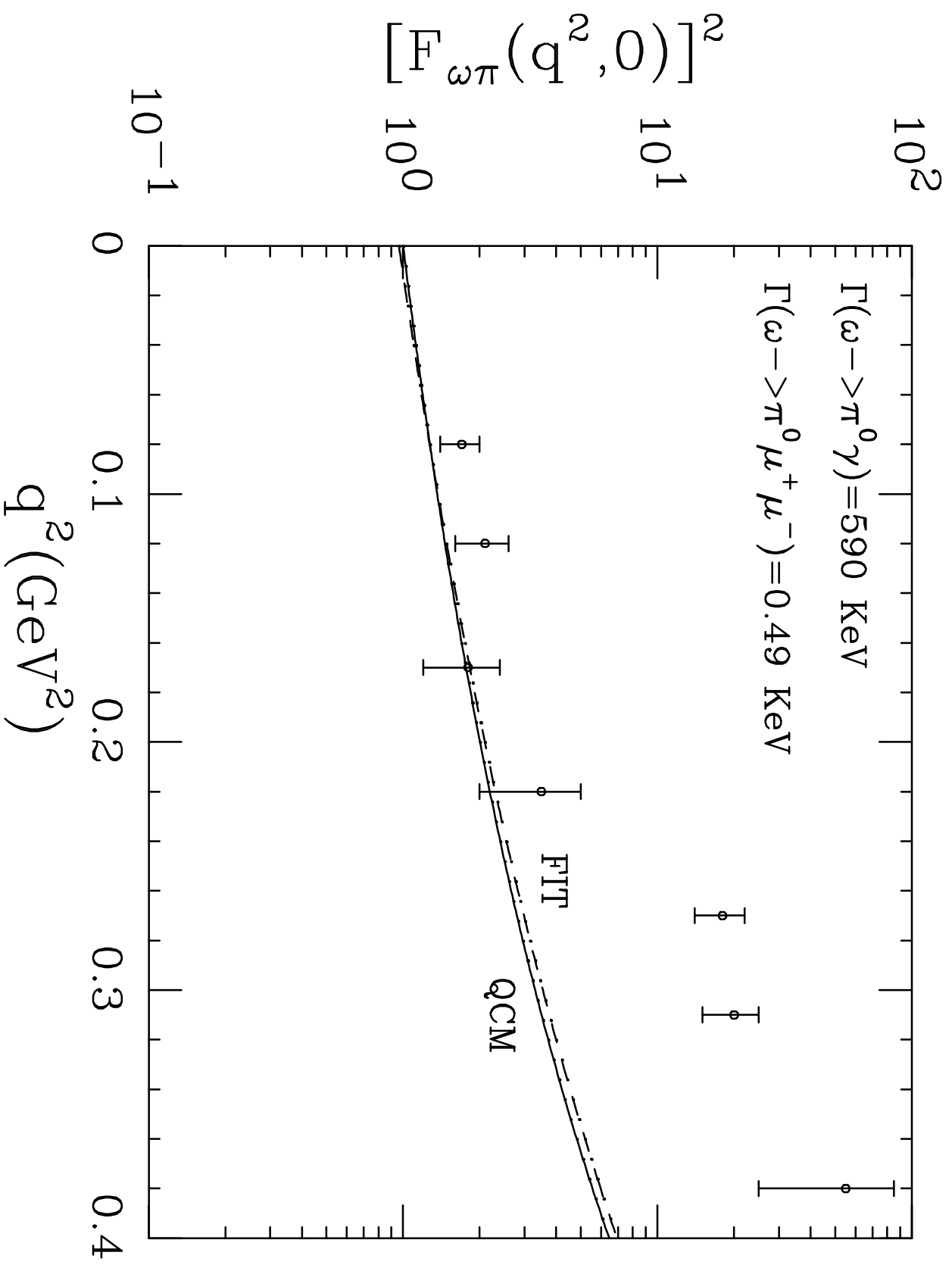


Fig. 5

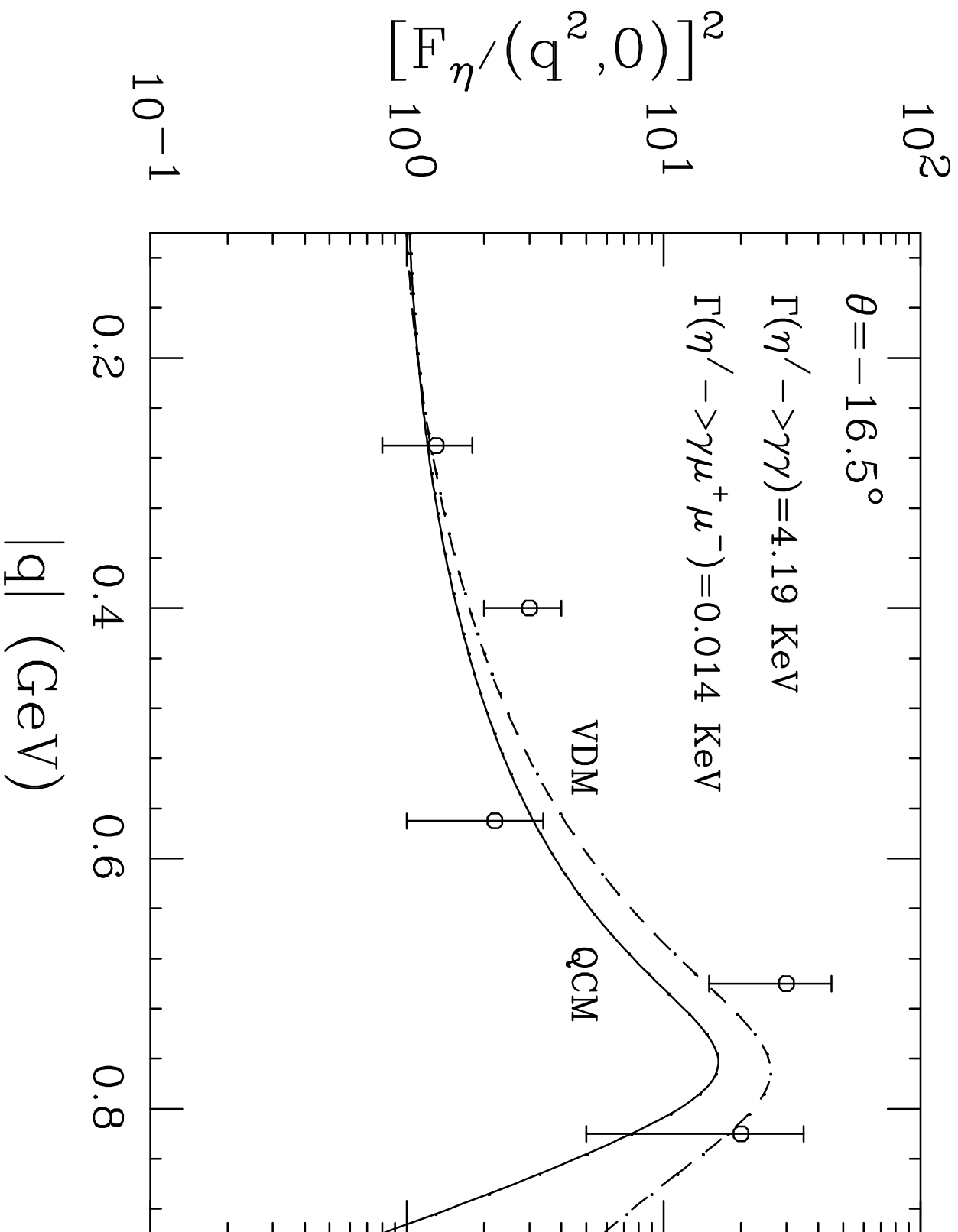


Fig. 6

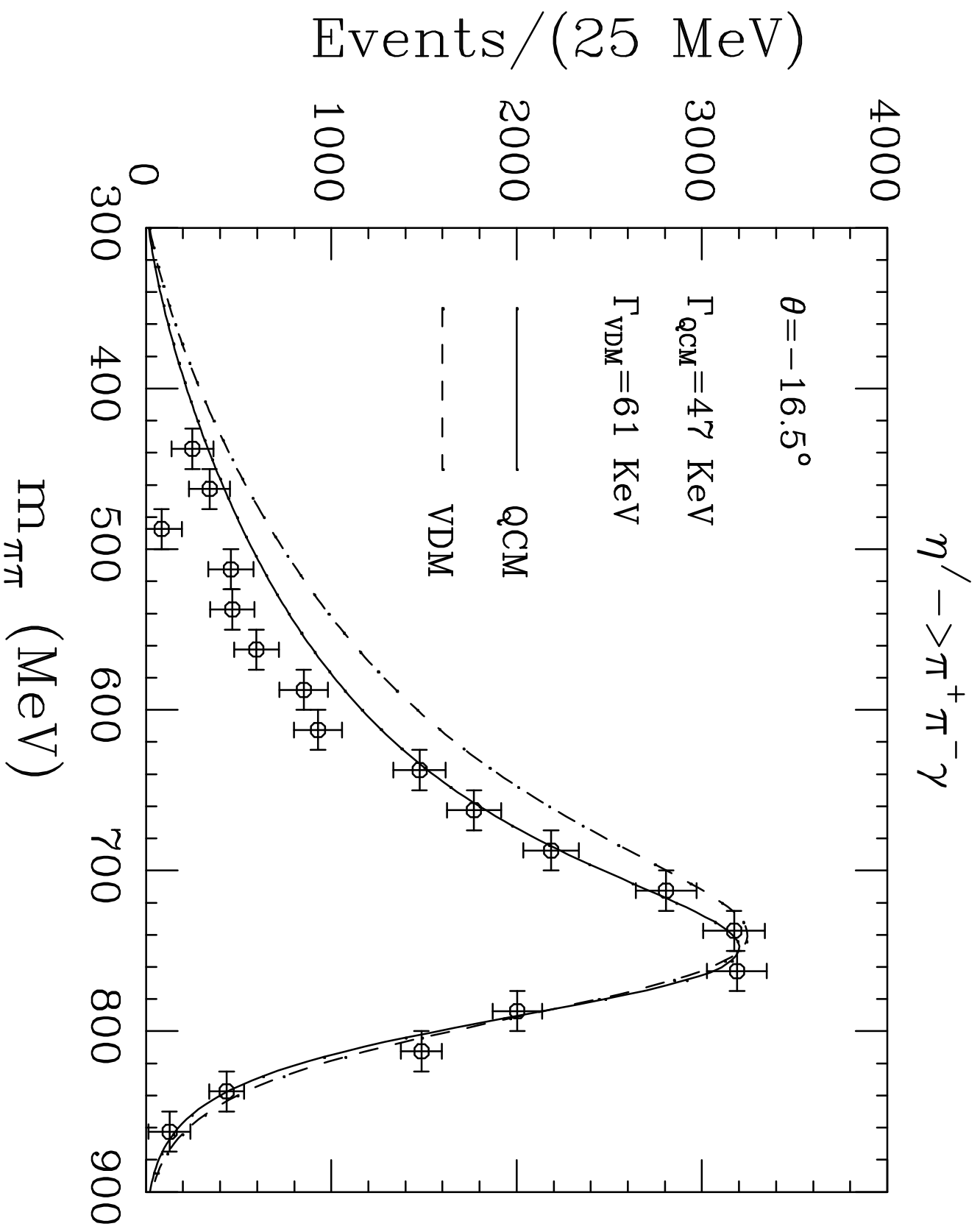


Fig. 7a

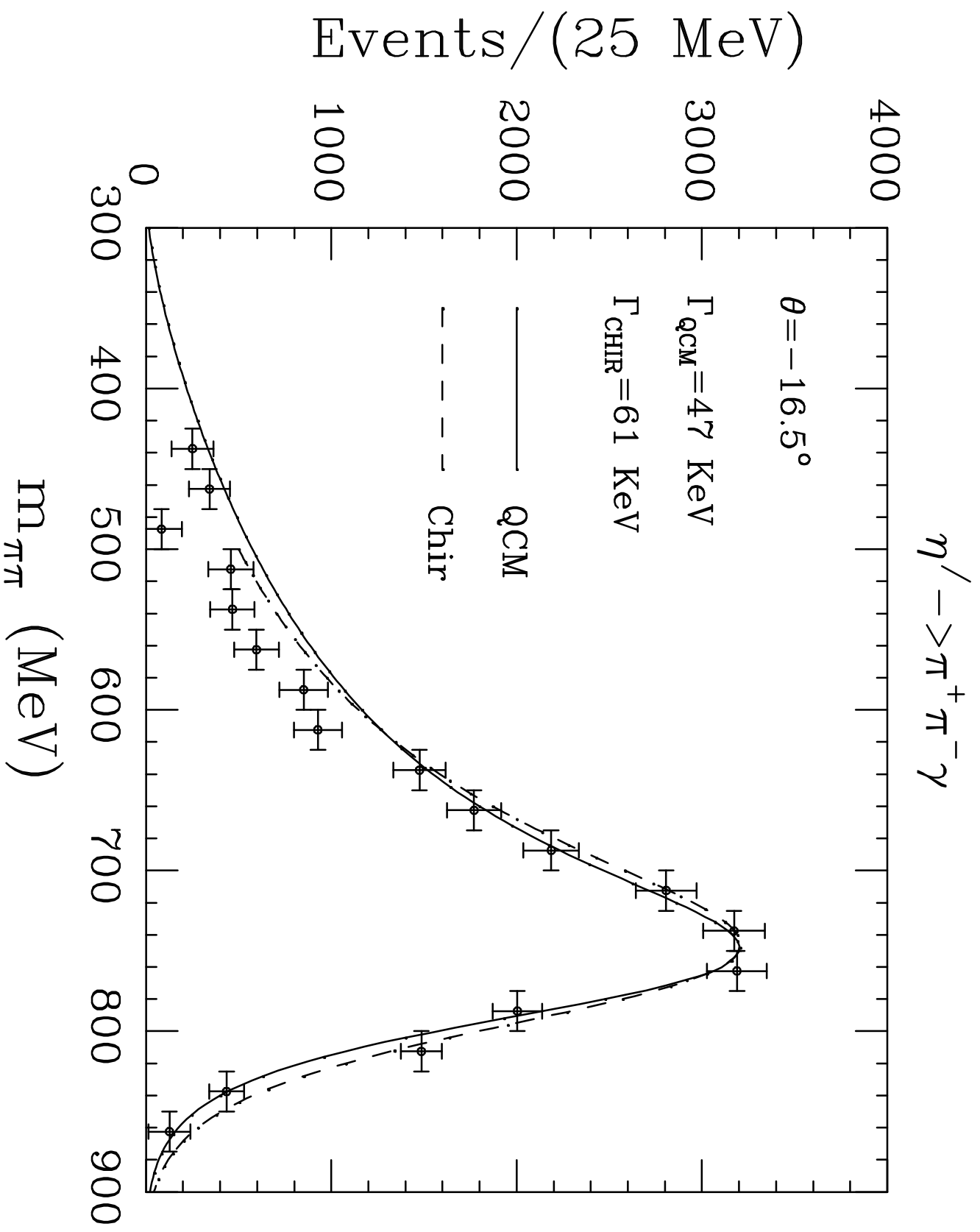


Fig. 7b

$\eta \rightarrow \pi^+ \pi^- \gamma$

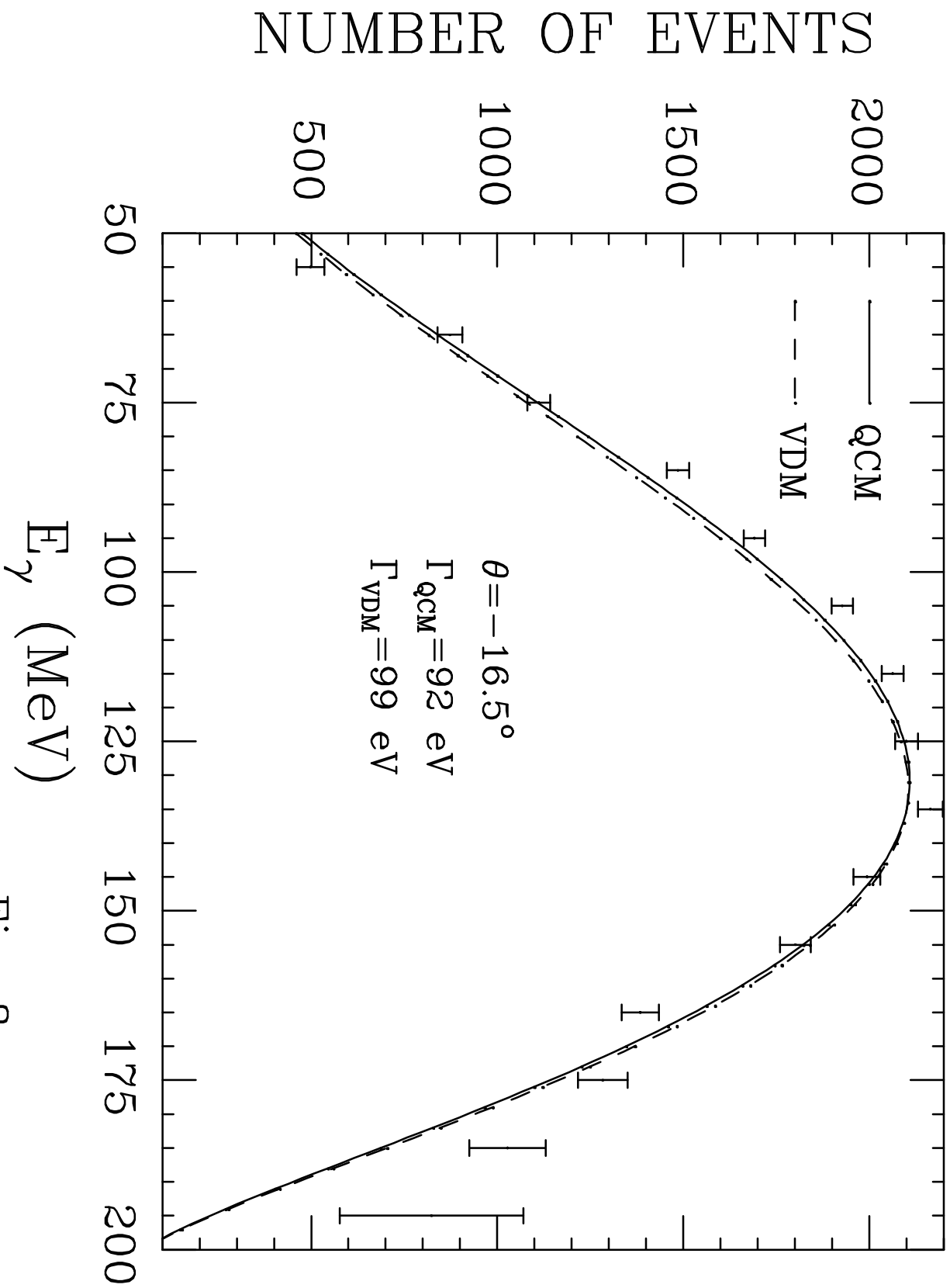


Fig. 8a

$$\eta \rightarrow \pi^+ \pi^- \gamma$$

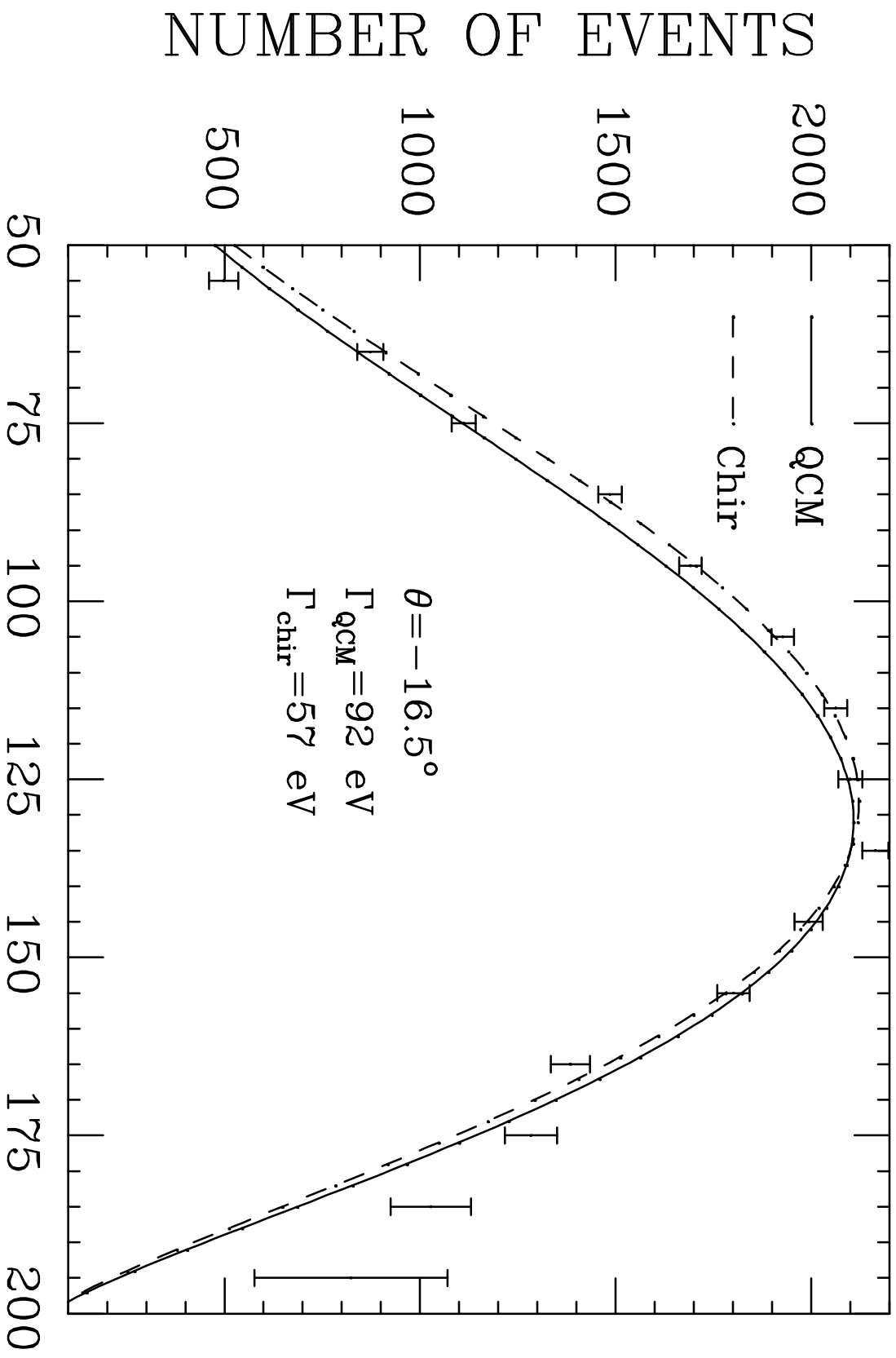


Fig. 8b

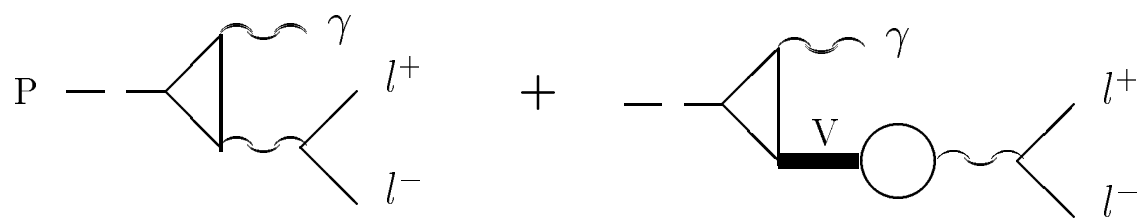


Fig. 1

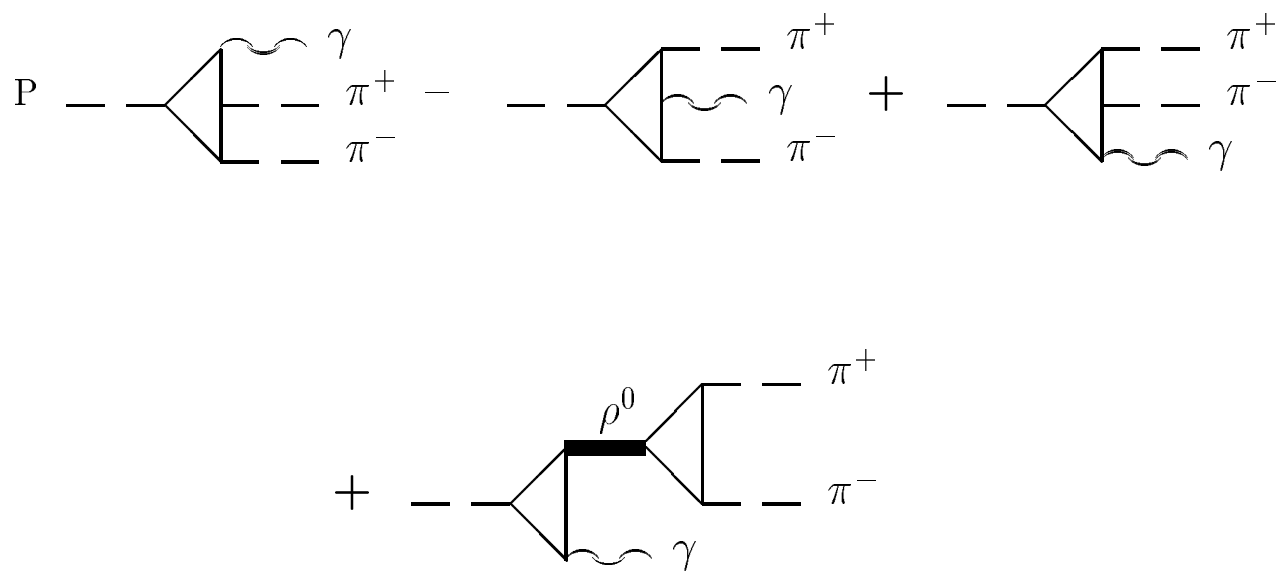


Fig. 2